Microstructure of Laser-Fired, Sol−Gel-Derived Tungsten Oxide Films

D. J. Taylor,*,† J. P. Cronin,‡ L. F. Allard, Jr.,§ and D. P. Birnie III†

Department of Materials Science and Engineering, University of Arizona, Tucson, Arizona 85721; Donnelly Corporation, Advanced Technology Center, 4545 E. Fort Lowell Road, Tucson, Arizona 85712; and High Temperature Materials Laboratory, Oak Ridge National Laboratory, Oak Ridge, Tennessee 37831

Received December 4, 1995. Revised Manuscript Received April 22, 1996⊗

Half-micron-thick tungsten oxide films were deposited by the sol−gel method onto indium tin oxide (ITO) coated soda lime silicate substrates. Following a 100 °C prebake, the samples were fired with a carbon dioxide laser at a variety of power densities and translation speeds. The laser-fired tungsten oxide films were characterized by spectrophotometry, electrochemistry, multiangle ellipsometry, and transmission electron microscopy and compared to similar furnace-fired films. The data showed an increase in electrochromic response with increased firing temperature up to the point where crystallization of the tungsten oxide retarded electrochromic response. A window with graded electrochromic properties was made by laser firing.

Introduction

After coating, sol−gel-derived films require heat in order to densify, which includes hydrolysis, completion of condensation reactions, network formation, organic burnout, and sintering. This heating is normally accomplished in a furnace. The disadvantage of furnace-firing is that the whole coated sample is subjected to the same firing temperature. Absorbed laser radiation provides another method of heating—one that is localized to the point of irradiation.[1,2] Laser densification of sol−gel-derived coatings has been shown to be successful for making hard, protective coatings[3,4] and optical waveguides.[5−8] The localized heat source that lasers provide has two advantages in firing sol−gel coatings: (1) the substrate may only be heated slightly, allowing low-refractory materials to be used as substrates; (2) the coating may be selectively heated. The latter consideration allows areas of the same coating to have different properties based on varied firing conditions. A pattern can be written into a sol−gel coating by densification with a laser, and the remaining undense coating can be easily etched away, leaving the pattern.[9] Or, one of the laser firing parameters can be changed continuously as the coated body is fired, producing a film with graded properties.

As reported in some of the electrochromic literature and in this work, firing conditions affect the electrochromic behavior of tungsten oxide. Through laser firing, the properties of sol−gel tungsten oxide can be tailored in several ways that are not possible by furnace firing. By taking some of the advantages of laser-fired, sol−gel-derived coatings and applying them to electrochromic films, patterns can be written into a tungsten oxide coating that will be electrochromic. The unfired sol−gel-derived tungsten oxide film does not exhibit electrochromism and etches orders of magnitude faster than the fired regions of the film. A sign or pattern that can be turned on or off can be laser written into the coating on a window. Also, since changing the firing conditions (e.g., incident laser power or translation speed of the laser beam) alters the microstructure, affecting the electrochromic behavior, coatings of graded electrochromic response can be made. Therefore, laser-fired tungsten oxide could be of interest for making graded electrochromic sunglasses, mirrors, or windows.

Tungsten oxide has been extensively studied for its electrochromic properties and potential commercial applications. These properties were first reported by Deb[10] in the late 1960s, and since then many theories have been proposed as to the electrochromic mecha-

† University of Arizona.
‡ Donnelly Corp.
§ Oak Ridge National Laboratory.
⊗ Abstract published in *Advance ACS Abstracts,* June 1, 1996.

(1) Chia, T.; Hench, L. L.; Qin, C.; Hsieh, C. K. Laser densification modeling. In *Better Ceramics Through Chemistry IV*; Zelinski, B. J. J., Brinker, C. J., Clark, D. E., Ulrich, D. R., Eds.; Mat. Res. Soc. Proc. Vol. 180; MRS: Pittsburgh, PA, 1990; pp 819−824.

(2) Taylor, D. J.; Birnie, III, D. P.; Fabes, B. D. Temperature calculation for laser irradiation of sol-gel films on oxide substrates. *J. Mater. Res.* **1995**, *10*, 1429−1434.

(3) Taylor, D. J.; Fabes, B. D.; Steinthal, M. G. Laser densification of sol-gel coatings, in *Better Ceramics Through Chemistry IV*; Zelinski, B. J. J., Brinker, C. J., Clark, D. E., Ulrich, D. R., Eds.; Mat. Res. Soc. Proc. Vol. 180; MRS: Pittsburgh, PA, 1990; pp 1047−1052.

(4) Taylor, D. J.; Fabes, B. D. Laser processing of sol-gel coatings. *J. Non-Cryst. Solids* **1992**, *147* and *148*, 457−462.

(5) Zaugg, T. C.; Weisenbach, L.; Fabes, B. D.; Zelinski, B. J. J. Waveguide formation by laser irradiation of sol-gel coatings. In *Submolecular Glass Chemistry and Physics*; Bray, P., Kreidl, N. J., Eds.; SPIE: Bellingham, WA, 1991; Vol. 1590, pp 26−35.

(6) Guglielmi, M.; Colombo, P.; Mancinelli Delgi Esposti, L.; Righini, G. C.; Pelli, S. Planar and strip optical waveguides by sol-gel method and laser densification. In *Glasses for Optoelectronics II*; Righini, G. C., Ed.; SPIE: Bellingham, WA, 1991; Vol. 1513, pp 44−49.

(7) Guglielmi, M.; Colombo, P. Mancinell Delgi Esposti, L.; Righini, G. C.; Pelli, S.; Rigato, V. Characterization of laser-densified sol-gel films for the fabrication of planar and strip optical waveguides. *J. Non-Cryst. Solids* **1992**, *147* and *148*, 641−645.

(8) Fabes, B. D.; Zelinski, B. J. J.; Taylor, D. J.; Weisenbach, L.; Boggavarapu, S.; Dent, D. Z. Laser densification of optical films. In *Sol-Gel Optics II*; Mackenzie, J. D., Ed.; SPIE: Bellingham, WA, 1992; Vol. 1758, pp 227−234.

(9) Fabes, B. D.; Taylor, D. J.; Weisenbach, L.; Stuppi, M. M.; Klein, D. L.; Raymond, L. J.; Zelinski, B. J. J.; Birnie, III, D. P. Laser processing of channel waveguide structures in sol-gel coatings. In *Sol-Gel Optics*; Mackenzie, J. D., Ed.; SPIE: Bellingham, WA, 1990; Vol. 1328, pp 319−328.

S0897-4756(95)00570-9 CCC: $12.00

nism.[11] In general, tungsten oxide colors by the reversible double insertion of an electron and a cation (e.g., H^+, Li^+, Na^+). In the fully oxidized state, it is colorless, and in the reduced state, a deep blue tungsten bronze is formed. Microstructure and morphology play a significant role in this intercalation process.[12] By controlling these parameters, one could design a material with optimal electrochromic behavior. This is an important factor in device design applications.

Initially, tungsten oxide was a candidate for electrochromic displays[13] but was never developed because of fast liquid-crystal displays (LCDs). Currently, a billion dollar market for electrochromic devices is predicted for the next 10 years.[14] They are presently used in sunglasses and automotive rear-view mirrors[15,16] and sunroofs.[17] Future applications include variable-tinted windows for automotive glass[17] and building windows.[18,19] Many researchers have built and tested whole electrochromic devices[20−23] with promising results. Several good review articles have been published recently on tungsten oxide[24] and electrochromism.[25−29] In this paper, we show the advantages of laser-fired, sol−gel-derived tungsten oxide films.

Experimental Section

Coating Preparation. The sol−gel precursor solutions were prepared by dissolving a peroxotungstic ester derivative in anhydrous ethanol (PTE/EtOH = 0.24 gm/mL). The precursor solution also contained 32 mol % oxalic acid dihydrate, where the concentration is referenced to the tungsten metal content in the PTE.[30−32] The coatings were deposited by dipping indium tin oxide (ITO) coated (12Ω/□) glass into the solution under ambient atmosphere and withdrawing at a rate of 28 cm/min. The coatings were then dried under controlled relative humidity at 100 °C for 1 h.

Laser Firing. The samples were fired by irradiation from a focused carbon dioxide laser, operated in continuous mode. The laser emission was Gaussian in profile. Beam diameters from 330 to 420 μm (measured at 1/*e*) were used to produce power densities between 3000 and 9400 W/cm^2. Translation speeds varied from 0.3 to 4 cm/s. Thermal modeling of these samples[2] indicated a maximum temperature rise from 200 °C to just over 400 °C. All of the electrochemical and microstructural analyses were performed on coatings which had been fired under chosen constant power and velocity conditions. In addition to these uniform coatings, we created a demonstration device with graded optical properties by varying the firing conditions across the sample. The laser power was held constant at 5.0 W while the translation speed was varied from 1.25 to 4.0 cm/s. Bands 0.4 cm wide were made at constant speed before incrementing the speed because of the small spot size of the irradiation.

Electron Microscopy. The structure of the tungsten oxide films was characterized using high-resolution transmission electron microscopy (TEM). Electron-transparent cross sections were prepared to permit observation of the film structure and interface structure. Two pieces of the WO_3/ITO/glass samples were glued together to form a sandwich with the films at the center. The sandwich was sliced perpendicular to the plane of the films, and the thin slice was dimpled and ion milled to make an area of tungsten oxide thin enough for good electron imaging. Analysis was carried out either on a Hitachi HF-2000 field emission analytical electron microscope (200 kV) or a JEOL 4000EX high-resolution transmission electron microscope (400 kV).

Optoelectrochemical Measurements. The electrochromic behavior of the laser-fired tungsten oxide films was tested by inserting them into a 1 cm^2 silica cuvette with a counter electrode (Pt wire) and a reference electrode (Ag/AgCl). The electrolyte in the cuvette was 0.01 M H_2SO_4. A standard three-electrode potentiostat maintained a constant voltage between the working electrode (i.e., the ITO/WO_3 sample) and the reference electrode by varying the current through the working electrode. The test cuvette was set inside a two-beam Perkin-Elmer spectrophotometer with a piece of ITO-coated glass in the same electrolyte placed in the reference beam. Transmission through the tungsten oxide films was measured at 550 nm while the potentiostat held the voltage at +0.5 V for 120 s (coloring) and −0.5 V for 60 s (bleaching). Transmission and current were recorded simultaneously as a function of time.

Current−voltage measurements were made using a standard sweep potential method. The potential was swept at 10 mV/s from +0.5 to −0.4 V while the current through the working electrode was recorded.

Results

Ellipsometry. Multiangle ellipsometry at 632.8 nm showed higher shrinkage and refractive index with more

(10) Deb, S. K. Novel electrophotographic system. *Appl. Opt.* **1969**, *suppl. 3.J*, 192−195.
(11) Granqvist, C. G. *Handbook of Inorganic Electroctrochromic Materials*; Elsevier: Amsterdam 1995.
(12) Monk, P. M. S.; Mortimer, R. J.; Rosseinsky, D. R. *Electrochromism: Fundamentals and Applications*; VCH: Weinheim, 1995.
(13) Faughnan, B. W.; Crandall, R. S. Electrochromic displays based on WO_3. *Top. Appl. Phys.* **1980**, *40*, 181−211.
(14) Cronin, J. P.; Agrawal, A. Large area transmissive electrochromic devices. To be published in the proceedings from the Symposium in Honor of Norbert J. Kreidl's Ninetieth Birthday, 1994.
(15) Baucke, F. G. K.; Duffy, J. A. Darkening glass by electricity. *Chem. Brit.* **1985**, *21*, 643−647.
(16) Kamimori, T.; Nagai, J.; Mizuhashi, M. Electrochromic devices for transmissive and reflective light control. In *Optical Materials Techology for Energy Efficiency and Solar Energy Conversion V*; Granqvist, C. G.; Ed.; SPIE: Bellingham, WA, 1986; Vol. 653.
(17) Lynam, N. R.; Agrawal, A. Automotive applications of chromogenic materials. In *Large Area Chromogenics: Materials & Devices for Transmittance Control*; Lampert, C. M., Granqvist, C. G., Eds.; SPIE: Bellingham, WA, 1989.
(18) Goldner, R. B.; Rauh, R. D. Electrochromic materials for controlled radiant energy transfer in buildings. In *Technology for Energy Efficient Solar Applications*; SPIE: Bellingham, WA, 1983; Vol. 428, pp 38−44.
(19) Svensson, J. S. E. M.; Granqvist, C. G. Electrochromic coatings for smart windows: Crystalline and amorphous WO_3 films. *Thin Solid Films* **1985**, *126*, 31−36.
(20) Passerini, S.; Scrosati, B.; Gorenstein, A.; Andersson, A. M.; Granqvist, C. G. An electrochromic window based on Li_xWO_3/$(PEO)_8$-$LiClO_4$/NiO. *J. Electrochem. Soc.* **1989**, *136*, 3394−3395.
(21) Kaneko, H.; Bessho, T.; Miyake, K. Properties of the symmetric tungsten oxide electrochromic cells. In *Electrochromic Materials*; Carpenter, M. K., Corrigan, D. A., Eds.; The Electrochemical Society Proceedings: Pennington, NJ, 1989; Vol. 90-2, pp 288−297.
(22) Ottermann, C. R.; Temmink, A.; Bange, K. Comparison of tungsten and nickel oxide electrochromism in single films and in all-solid-state devices. *Thin Solid Films* **1990**, *193/194*, 409−417.
(23) Jelle, B. P.; Hagen, G.; Sunde, S.; Ødegård, Dynamic light modulation in an electrochromic window consisting of polyaniline, tungsten oxide and a solid polymer electrolyte. *Synth. Met.* **1993**, *54*, 315−320.
(24) Granqvist, C. G. Electrochromic tungsten-oxide-based thin films: Physics, chemistry and technology. *Phys. Thin Films* **1993**, *17*, 302.
(25) Deb, S. K. Some aspects of electrochromic phenomena in transition metal oxides. In *Electrochromic Materials*; Carpenter, M. K., Corrigan, D. A. The Electrochemical Society Proceedings: Pennington, NJ, 1989; Vol. 90−2, pp 3−13.
(26) Donnadieu, A. Electrochromic Materials. *Mater. Sci. Eng.* **1989**, *B3*, 185−195.
(27) Gambke, T.; Metz, B. Electrochromic layers for active optical filters; *Glastech. Ber.* **1989**, *62*, 38−45.
(28) Granqvist, C. G. Electrochromism and smart window design. *Solid State Ionics* **1992**, *53−56*, 479−489.
(29) Deb, S. K. Opportunities and challenges of electrochromic phenomena in transition metal oxides. *Solar Energy Mater. Sol. Cells* **1992**, *25*, 327−338.
(30) Cronin, J. P.; Tarico, D. J.; Agrawal, A.; Zhang, R. L. U.S. Patent 5,252,354, 1993.
(31) Cronin, J. P.; Tarico, D. J.; Agrawal, A.; Zhang, R. L. U.S. Patent 5,277,986, 1994.
(32) Denesuk, M.; Cronin, J. P.; Kennedy, S. R.; Law, K. J.; Nielson, G. F.; Uhlmann, D. R. Coloration behavior of hybrid electrochromic films. In *Optical Materials Technology for Energy Efficiency and Solar Energy Conversion XIII*; Wittwer, V., Granqvist, C. G., Lampert, C. M., Eds.; SPIE: Bellingham, WA, 1994; Vol. 2255.

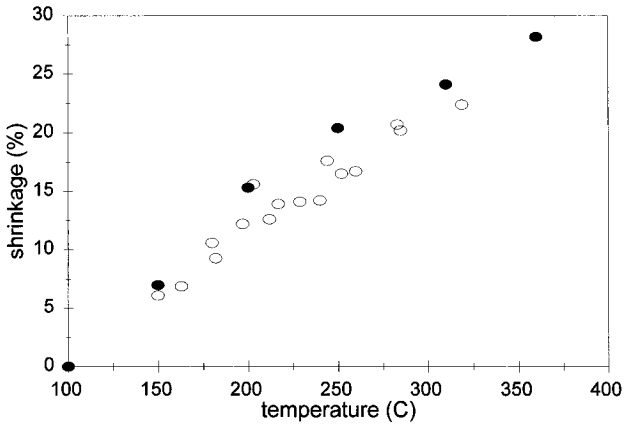

Figure 1. Shrinkage of laser-fired and furnace-fired, sol−gel-derived tungsten oxide films as a function of firing temperature. Open circles denote laser firing and filled circles indicate furnace firing. Temperatures of laser-fired samples are calculated from thermal modeling and represent the peak temperature reached during the firing event.

Table 1. Shrinkage and Refractive Index of Sol−Gel-Derived Tungsten Oxide Films as a Function of Firing Conditions[a]

firing method	temp (°C)	shrinkage (%)	refractive index
prebake only	100	0	1.95
laser	285[b]	20.2	2.08
furnace	310	24.1	2.07
laser	320[b]	22.4	2.11
furnace	360	28.2	2.13

[a] At similar refractive indexes, the firing temperatures and shrinkages are lower for laser-fired films than for furnace-fired films. [b] Calculated temperatures.

incident laser power and slower translation speeds (i.e., higher temperature and longer firing times). Laser-fired tungsten oxide films were 400−500 nm thick depending on firing conditions. Shrinkage varied with firing temperature as shown in Figure 1. The increase in refractive index that accompanied the increase in film shrinkage indicated densification of the films rather than ablation, as shown in Table 1. The index of refraction is similar for the highly crystallized laser-fired films (at 22% shrinkage) and furnace-fired films (at 28% shrinkage); however, the laser-fired film is less dense than the furnace-fired film.

Electron Microscopy. High-resolution transmission electron microscopy revealed crystallite size and orientation, when present, and relative volume fraction of the crystals. Some laser-fired sol−gel-derived tungsten oxide films were amoprhous (Figure 2) and others were highly crystalline (Figure 3). The film shown in Figure 2 was fired at a high translation speed (4 cm/s), which relates to a firing time of 3 ms. The irradiation was sufficient to provide densification in the short time of the high-speed laser pass. The highly crystalline film shown in Figure 3 was fired at a much slower speed (i.e., 1 cm/s) than the film in Figure 2, with a firing time of 18 ms. The lower translation speed produces a higher firing temperature and a longer firing time, which together are responsible for the difference in microstructure.

The size of the crystallites in films with ≳0.7 volume fraction crystalline phase was approximately 20−50 nm. Crystallites as small as 4 nm could be seen in otherwise amorphous films. Figure 3 shows a film that is fully crystalline with large, adjacent crystals. Figure 4 shows

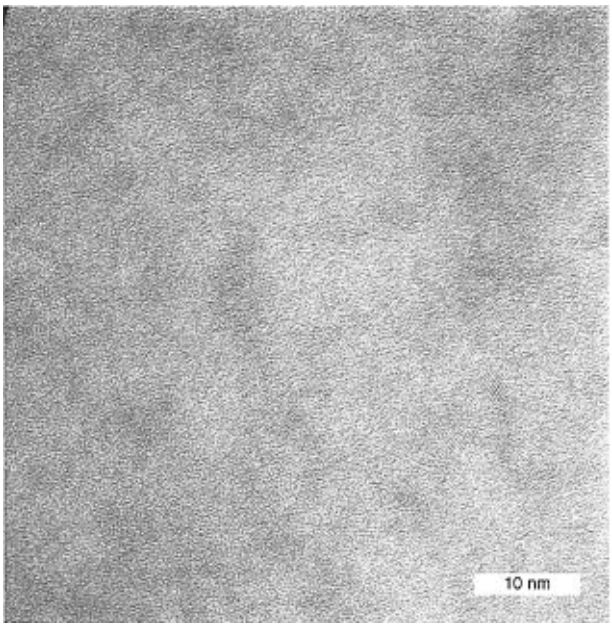

Figure 2. TEM micrograph of a sol−gel-derived tungsten oxide film fired with a carbon dioxide laser at 6 Watts and 4 cm/s. A few, small (2−5 nm) crystallites can be seen in an otherwise amorphous microstructure.

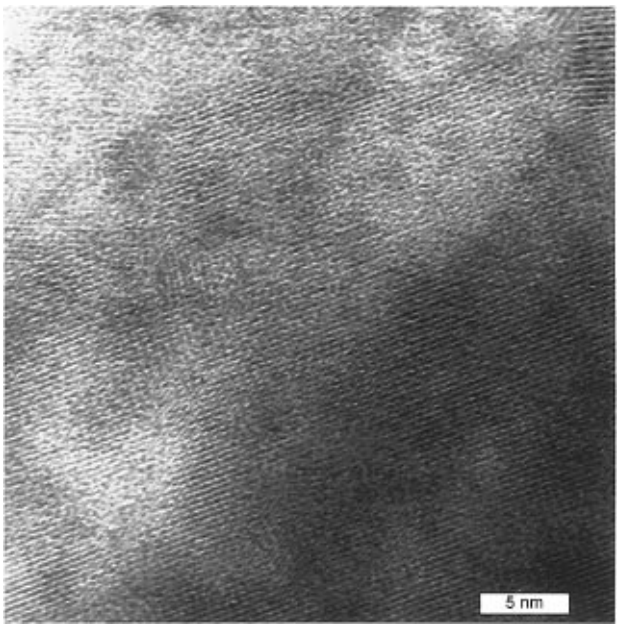

Figure 3. TEM micrograph of a sol−gel-derived tungsten oxide film fired at 4 W and 1 cm/s that produced a highly crystalline microstructure.

a film that has many smaller crystals surrounded by amorphous regions. All of the crystallites appeared to be randomly oriented with respect to the substrate (crystalline ITO) and to each other. Most of the films examined with TEM showed an amorphous matrix of tungsten oxide with randomly dispersed crystallites that ranged from 5 to 20 nm in diameter. These partially crystalline films were produced at medium firing conditions.

Electrochemical Analysis. Step potential measurements showed films with a wide range of coloring and bleaching behavior. Initially, the transmissivity of the tungsten oxide films decreased as the +0.5 V potential (with respect to Ag/AgCl) is applied. Coloration is due to the intercalation of charge into the

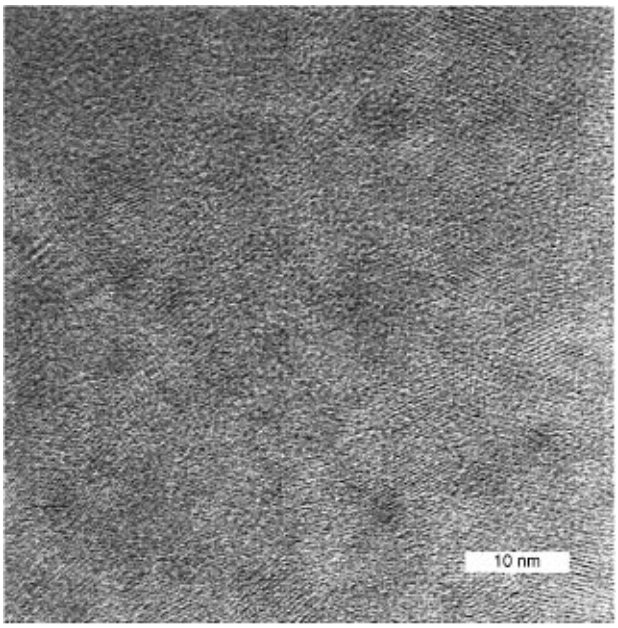

Figure 4. TEM micrograph of a laser-fired (6 W and 0.7 cm/s), sol−gel-derived tungsten oxide film exhibiting a high volume fraction of 10−15 nm crystallites randomly distributed in an amorphous matrix.

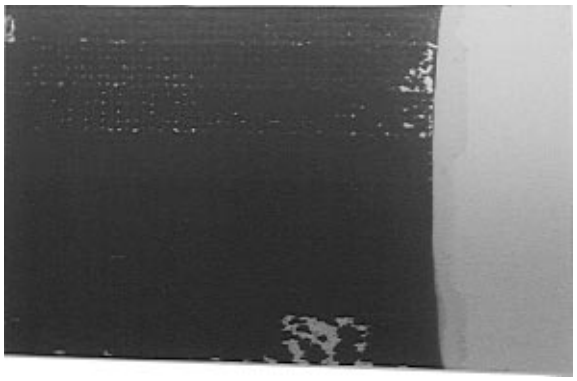

Figure 5. Photograph of a window with graded electrochromic response that was made by laser firing a sol−gel-derived tungsten oxide film on ITO-coated glass. Note the delamination of the film on the dark edge of the sample that occurred during electrochemical cycling. This was the side that was fired at the lowest translation speed, 1.25 cm/s (i.e., reached the highest temperature), just above the damage threshold for laser firing. The spottiness on the light side may be due to etching from the electrolyte in the least dense part of the film.

tungsten oxide film. After 2 min, the polarity of the applied potential was reversed and the tungsten oxide bleaches, ejecting charge from the film. The bleached films were similar to their initial state. The range of optical responses which was achieved can be emphasized by examining our gradient-optic demonstration window (Figure 5). Here, the range of velocities used started with firing conditions which caused rather little coloration and continued up to firing conditions which ultimately caused damage (details in the Experimental Section). The following additional electrochemical analyses were performed only on uniformly fired coatings to ensure that the structures were representative of specific known temperature exposures.

Figure 6 shows the current−voltage (c−v) measurements of an amorphous (micrograph in Figure 2) and of a crystalline (micrograph in Figure 3) laser-fired, sol−gel-derived tungsten oxide film. The rest potential was

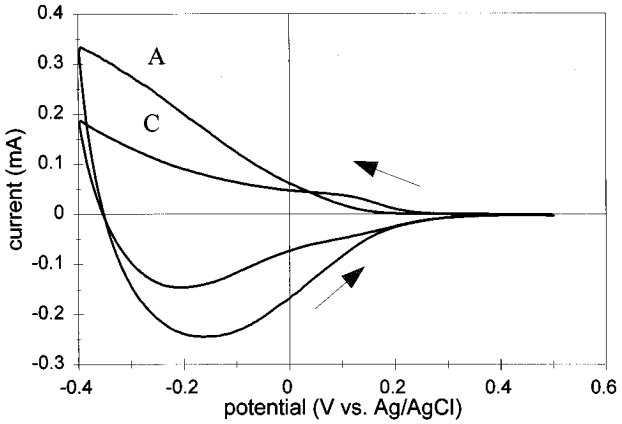

Figure 6. Current−voltage curves for amorphous (A) and crystalline (C) laser-fired, sol−gel-derived tungsten oxide films.

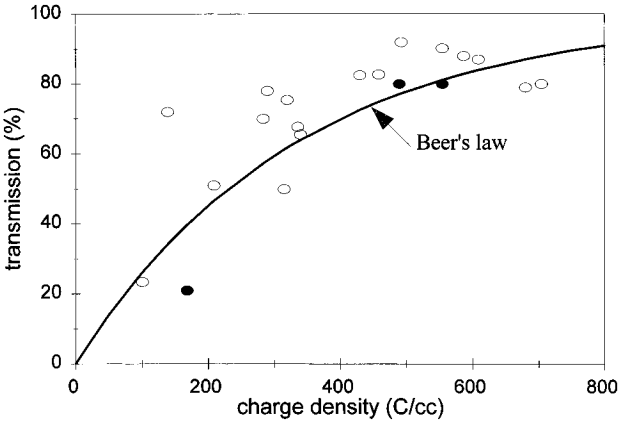

Figure 7. Optical modulation expressed as percent transmission at 550 nm versus intercalated charge density (in C/cm^3) for laser-fired, sol−gel-derived tungsten oxide films. The filled points represent data from furnace-fired films. The Beer's law curve is $[1 - \exp(-c\alpha x)]$, where c is concentration, α is absorptivity, and x is film thickness. Errors occur between the data and the curve because an average constant value for film volume and efficiency is assumed in calculating absorptivity used to plot the curve.

0.251 V for the amorphous material and 0.045 V for the crystalline material (versus Ag/AgCl) and were accounted for in plotting the data. The c−v curve from the film with the amorphous microstructure exhibits a larger charge capacity than that of the film with a crystalline microstructure. Less charge is intercalated into the crystalline film, and an inflection in the c−v curve at $x = 0.15$ V shows evidence of another reaction during coloring, which is not evident in the c−v curve for the amorphous material and is not reversible. From other data, we would expect higher optical density from the amorphous films at the same voltage due to the larger intercalated charge (Figure 7). However, optical density was not measured concurrently with current during the c−v measurements.

Long-term cycling of the laser-fired films was not done to determine durability and device lifetime in an acid medium. Similar coatings that were furnace-fired and tested in acidic electrolyte indicate that the crystalline film is more durable than the amorphous. The higher density crystalline film is more chemically stable to the acidic electrolyte. Longer cycle life is attributed to this and not to better expansion/contraction characteristics during intercalation.

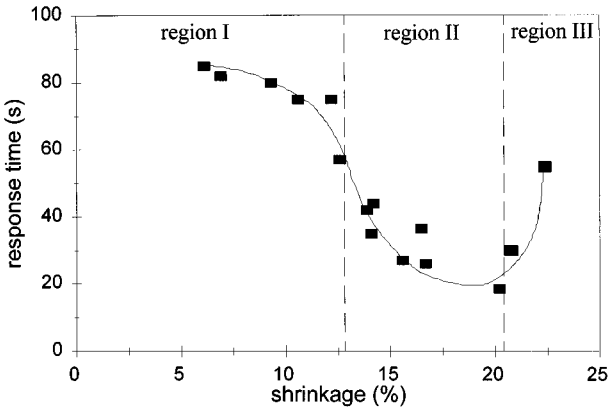

Figure 8. Response time for coloration versus shrinkage in laser-fired tungsten oxide films. Response time is determined by the amount of time required to color 90% of the modulation at 550 nm. Each sample colors for 120 s at 0.5 V referenced to Ag/AgCl. Region I indicates an amorphous film microstructure (Figure 2), while those of region II are partially crystalline (Figure 4). The films in region III are highly crystalline (Figure 3).

Modulation (the optical change between colored and bleached states) increased with intercalated charge to a maximum value before a further increase in charge made little optical change, as seen in Figure 7. Optical absorption should increase as the concentration of color centers in the tungsten oxide film increases. Beer's law is used to calculate absorption: $I/I_0 = \exp(-c\alpha x)$, where c is the concentration of the absorbing species, α is absorptivity, and x is the thickness of the layer. To calculate a single Beer's law curve, film thickness, film area, and optical efficiency are assumed constant. Since each sample has a unique area, thickness, and optical efficiency, scatter will occur between the data and the Beer's law curve. The Beer's law curve shown in Figure 7 is in terms of transmission (i.e., $1-I/I_0$) and is meant to show absorption behavior rather than to fit the data points.

Figure 8 shows time to color (90% of total modulation at 550 nm, with 120 s coloration time) as a function of shrinkage where the time to color decreases with increasing shrinkage to a minimum before increasing. The graphed data are divided into three regions. The response time of films with low shrinkage is relatively slow (region I). As shrinkage increases, response times are seen to decrease (region II), demonstrating enhanced electrochromic behavior. At higher shrinkages (region III), time to 90% coloration increases. By this data, optimal electrochromic performance is seen to occur at less than full densification, indicating several competing mechanisms influencing electrochromism.

Discussion

Maximum shrinkage is higher for furnace-fired films due to the much longer firing times. With furnace firing, all processes are given sufficient time to equilibrate at a given temperature, thereby reducing the importance of time as a variable. However, laser firing provides rapid heating—holding a spot near the maximum firing temperature for tens of milliseconds—making kinetics important. For these reasons, the microstructure of a laser-densified and a furnace-densified sol–gel-derived tungsten oxide films could be different for a given shrinkage or refractive index.

The time near the maximum firing temperature from laser heating depends on the translation speed of the sample. With rapid firing, small differences in firing times can make large differences in the densification of sol–gel films. Therefore, reporting only firing temperature presents only part of the firing profile, but it is the way in which we can compare laser-fired samples to furnace-fired samples, which are obviously denoted by furnace temperature. As seen in Figures 2–4, crystallization occurs in the samples fired at low translation speeds (i.e., 0.7–1 cm/s) and not in the sample fired at 4 cm/s, which has a firing time 6 times shorter than that of the crystallized samples. The kinetics of these samples are not directly comparable because they were fired at different power densities. Crystallization kinetics of tungsten oxide can be studied by comparing samples fired at different translation speeds while maintaining a constant laser-firing temperature. This would be accomplished by defocussing the laser beam to offset the temperature rise associated with decreasing translation speed. However, such kinetic studies are beyond the scope of this paper.

The firing temperature and firing time affects the electrochromic performance of sol–gel-derived tungsten oxide films. By examining the structure, we have an idea of how this processing–property relationship works. Transmission electron microscopyy is an excellent technique for directly observing the microstructure of the films, and it helps us to elucidate the structure–property relationship. Next, we discuss the effect of processing conditions on microstructure and how it influences electrochromism in laser-fired, sol–gel-derived tungsten oxide films.

At low firing conditions, optical modulation is barely noticeable, due to an incomplete tungsten oxide network and a large amount of retained organics. Organic molecules bonded to tungsten ions inhibit the formation of color centers by these ions. This stage of firing is noted in region I of Figure 8 and corresponds to the microstructure seen in Figure 2. As firing conditions increase (i.e., increased firing temperature and/or increased firing time, although still on the order of tens of milliseconds) oxide network formation proceeds and organics are evolved, which is accompanied by better electrochromic behavior. The response time, which is an indicator of electrochromic behavior, decreases during this stage of firing, as seen in region II of Figure 8. When burnout is complete and the structure is still porous, electrochromism is maximized (Figure 4). At higher firing conditions, optical modulation decreases and response times increase (region III in Figure 8), which is coincident with crystallization (Figure 3). Microstructurally, good ion and electron transport (i.e., diffusion) is enhanced by an open structure and slowed in high density or crystalline regions. When small crystallites are dispersed in an amorphous matrix, electrochromic properties vary between the two extremes depending on the degree of crystallinity and density of both phases. Therefore, optimal electrochromic properties of the sol–gel-derived tungsten oxide films are a balance among network formation, organic burnout, porosity, and crystallization.

The decrease in electrochromic behavior associated with crystallization is a well-known effect;[33−35] however, many still speculate as to the reason. As tungsten oxide crystallizes, it changes its electronic structure from tungsten ions with localized charge carriers to a Drude-type metallic tungsten bronze.[33] Small polaron absorption is thought to be responsible for coloration in amorphous tungsten oxide films. On the other hand, with crystallization the structure not only becomes ordered but increases in density, which is known to inhibit electrochromism. The data here suggest the decrease in electrochromic response is due more to the microstructure than to local electronic states. Probably due to the short firing times involved, less shrinkage is achieved with laser firing than is observed for similar furnace-fired films. However, TEM micrographs show that crystallinity exists as small crystallites dispersed in an amorphous matrix of tungsten oxide and not as a continuous crystalline phase. A simple rule of mixtures would explain the increase in refractive index from the onset of crystallization at higher firing conditions, while the fact that there is less amorphous material with fewer sites available for coloration would explain the decrease in optical modulation. Highly crystalline films that have higher refractive indexes and presumably higher densities exhibit electrochromic behavior, albeit worse than the amorphous films. We can conclude that crystallinity does not prohibit electrochromism[33] and that the decrease in modulation and response times is a result of the microstructure. However, we cannot rule out differences in electronic states that occur in the different phases.

More complicated behavior arises when the crystalline and amorphous phases are mixed in a single tungsten oxide film. Only once[32] in the literature have researchers reported on a mixed amorphous/crystalline microstructure in tungsten oxide films. In that study, the chemistry of the precursor solution was altered to change the microstructure of the tungsten oxide films, while the firing schedule was held constant. Films made with oxalic acid in the precursor were partially crystalline, while those made without were amorphous. Many have studied crystalline and amorphous films, usually as measured by X-ray diffraction (XRD); however, XRD cannot distinguish low-to-medium volume fractions of crystallinity in thin tungsten oxide films when nanometer-sized crystals are present. Instead of considering only the extremes of crystallinity, we must now think in terms of volume fraction crystallinity, and size and orientation of crystallites.[32,35]

Conclusion

Electrochromic windows with good properties were made by laser firing sol-gel-derived tungsten oxide films. Changing the laser power density and the translation speed of the sample affected the amount of densification, and therefore the electrochromic behavior of the films was changed. By continual variance of the laser firing parameters over the area of densification, coatings of graded performance were made. Depth of coloration increased with intercalated charge density. Response speed increased with increasing densification until the films were highly crystallized, at which point the response slowed substantially.

Acknowledgment. The authors are grateful for collaboration and discussions with D. R. Uhlmann and B. D. Fabes which occurred in the early stages of this research project. In addition we appreciate the help of S. R. Kennedy for all his help in preparing the sol−gel tungsten oxide films and C. L. Smith for her help in printing the micrographs and acting as a liason between the authors. This research was supported by the Donnelly Corp. and by the U.S. Department of Energy, Assistant Secretary for Energy Efficiency and Renewable Energy, Office of Transportation Technologies, as part of the High Temperature Materials Laboratory Fellowship Program, under Contract DE-AC05-840R21400 managed by Lockheed Martin Energy Systems.

CM950570B

(33) Schirmer, O. F.; Wittwer, V.; Baur, G.; Brandt, G. Dependence of WO_3 electrochromic absorption on crystallinity. *J. Electrochem. Soc.* **1977**, *124*, 749−753.

(34) Cronin, J. P.; Tarico, D. J.; Tonazzi, J. C. L. Agrawal, A.; Kennedy, S. R. Microstructure and properties of WO_3 films made by the sol-gel process for large area electrochromic windows. In *Sol-Gel Optics II*; Mackenzie, J. D., Ed.; SPIE: Bellingham, WA, 1992; Vol. 1758, pp 343−359.

(35) Taylor, D. J. Structure and properties of laser-fired, sol-gel derived tungsten oxide films. Ph.D. Dissertation, University of Arizona, Tucson, AZ, 1995.